TEST OBSERVATIONS OF CLOUDSAT

D.Morris, G.Butin, N.Marcelino *
IRAM, 38406 St. Martin d'Heres,
France.,

May 30, 2008

Abstract

Test observations to assess the risk of interference due to Cloudsat emissions were made at the IRAM 30m telescope in July 2006. The telescope was pointed at various offsets from the predicted culmination of Cloudsat and short integrations were made. A simple axially symmetric model of the antenna sidelobe patterns was used to predict an upper limit to the expected signal. Although interference in the shared band was detected, it is of short duration. In routine astronomical observations its impact can be reduced by telescope pointing restrictions during satellite transits and by avoiding observations when the satellite is near the zenith. The loss of observing time will be small. In this special case (time) sharing between Radioastronomy and an active service is feasible at the price of some loss in observing time. This is possible because only one fast moving satellite with excellent sidelobes in angle and frequency is active.

1 INTRODUCTION

Cloudsat is the last of 5 satellites in the "A-Train" [1] launched (28 May 2006). This is a constellation of earth observation satellites in low earth orbit (equatorial altitude 705 km). All 5 are in essentially the same sun-synchronous orbit and pass a given point within 17 minutes. Cloudsat with its 94.05 GHz radar is one of two "active" satellites in the constellation - Calipso has a lidar. As its name implies Cloudsat is a cloud profiling radar which is designed to probe the density of cloud droplets as a function of height. This requires a high effective peak radiated power ($\geq$ 1 GW !). The problems posed for Radioastronomie , and in particular for the ALMA project, have been described in the ALMA report 504 (2004). The other 3 satellites use a variety of passive sensors at microwave, optical and infra-red wavelengths. The orbit of Cloudsat has been chosen to scan a grid parallel to but offset 215 km east, at the equator, from the Worldwide Reference System 2, Figure 1. This takes 233 orbits to complete (about 16 days), after which

* IRAM, 18012 Granada, Spain

the scanning process repeats. The orbits of the satellites are corrected from time to time so that their track does not deviate more than 20 km from their grids. This translates to an uncertainty in elevation of about 2 degrees. Figure 2 is an illustration of the type of data provided by Cloudsat. It shows the transit of Cloudsat over the eye of the hurricane "Bud".

Durden and Boain have described the satellite [2]. It transmits in a 100 MHz band with a Primary Allocation to "Space Research (active)" which is shared with Radioastronomy. Details of the radiated beam and its spectrum are reproduced in Figures 3 to 6. Over land the transmitted beam is directed to the local nadir with a precision of about 0.07+-0.05 degrees (comparable to the transmitter half power beamwidth of 0.11 degree). Pulses of width 3.3 microseconds are transmitted at a rate of about 4 KHz. Their rise and fall times are 50 ns and 23 ns respectively. The bandwidths are given as 300 KHz (-3 dB), 2 MHz (-20 dB), 80 MHz (-60 dB). Any spurious radiation is believed to be $\leq -40dBc$, harmonics $\leq -50dBc$ (second), and $\leq -60dBc$ (third). Polarization is linear (orientation unknown to IRAM). The peak and average pulse powers are 1800 and 25 watts. The transmitting antenna has a maximum gain of 64 dBi with very low sidelobes.

While there is general agreement that its radiation may destroy any SIS radioastronomy receiver on the IRAM 30m telescope when optimally coupled to its beam ("main beam - main beam"), the implications for routine radioastronomy observations are uncertain. The purpose of the present tests was to quantify the danger of interference at frequencies away from 94 GHz and with coupling other than "main-beam to main-beam". In fact we were not able to check satellite main-beam to telescope sidelobes coupling since this requires transits which pass very close to the zenith, which are rare.

2 CLOUDSAT OVERPASSES AND SIGNAL PROPERTIES

The typical properties of the overpasses during a 16 day cycle have been calculated using the "predict" software [6]. There are 2 or 3 significant passes twice per day. They are displayed in Figures 7, 8, 9, 10. Figure 7 shows that Pico Veleta, the site of the IRAM 30m radio telescope, is sufficiently close to the grid of the World Reference System that Cloudsat can pass within a very few degrees of the zenith. The signal strength (Figure 8), expressed as the power received by an isotropic antenna, was calculated using a model transmitter sidelobe pattern (see Figure 29) which was essentially an upper envelope of the published pattern (Figure 6) [2]. A more typical power might well be 10-15 dB weaker depending on exactly where the sidelobes are scanned.

3 OBSERVATIONS

Since the angular velocity of Cloudsat is typically many times the sidereal rate (Figures 9, 10), it is impossible to track it with the IRAM 30m telescope. Hence for each pass that we observed we placed the telescope beam at an, in principle, known distance from the culmination position (closest approach). In planning we used the NASA "Overpass Predictor" to position the

telescope. This gives values with a precision of 0.01 degrees, about 1.3 half power beamwidths of the 30m telescope at 94 GHz. In fact the accuracy is apparently worse, and this makes an exact interpretation the results difficult ! In subsequent analysis we have preferred the results from the "clsat" program developed by Juan Penalver [5] which uses a well described algorithm and has high time resolution. In this respect it is superior to "predict" [6]. Their predictions differ slightly, even when using the same orbital parameters (the "two line element" values provided by NASA) and observatory coordinates. Figure 11 shows a comparison for scan 26. The elevations, in degrees, at closest approach are 86.0169 (clsat), 86.0507 (predict) and 85.592 (Overpass Predictor). Spectral data were taken as for an "on the fly" observation so that the telescope scanned a small distance in azimuth instead of being stationary. This scan distance varied in the range 10-720 arc seconds during the session. The 100 KHz, 1 MHz and 4 MHz filter backends were used. The local oscillator was set to get 94.05 GHz at mid spectrum. No attempt was made to observe the higher harmonics, which are expected to be 50 dB weaker. Integration time per spectrum was in the range 0.05-0.5 seconds, since the satellite is expected to cross the telescope beam in a fraction of a second.

We attempted to observe 12 overpasses, details of which are given in Table 1. This gives date and scan number, telescope azimuth and elevation, the predicted position of nearest approach from the JPL Overpass Predictor, and that derived from "clsat". There follows the elevation difference telescope-clsat prediction, the scan length, sample time and spectral resolution.

4 ANALYSIS

We have tried to interpret the results in terms of a simple model for the sidelobe response of the 30m telescope and the transmitter. In both cases only worst case evaluations are possible. The exact pointing of the transmitter beam in unknown at any instant, the sidelobes of the 30m telescope have not been measured at 94 GHz, and the track of the satellite is only known approximately.

In 3 favorable cases (strong signal) where the spectral peak has been resolved as a function of time it has been possible to approximately "fit" the observed signal as a function of time with a model for the 30m sidelobe response. The spectra and fit are shown in Figures 16 - 18 where the abscissa has been labelled in angular measure calculated from the theoretical angular speed of Cloudsat. An attempt to identify sidelobe responses was also possible for scans 26 and 99 (Figure 12, 13). The remaining unresolved spectra are displayed in Figures 23 - 27. The model is for a telescope with gaussian illumination (taper -14 dB), blockage by focus cabin and supports, and random panel errors of rms 53 microns. Such a simple model acounts quite well for the inner sidelobes (Figures 20, 21). It is compared with the ITU model Rec.S149 in Figure 19. But there are other known sources of sidelobe radiation which must be considered. Firstly, spillover around the subreflector beginning at 2.8 degrees from boresight. Its peak is +15 dBi. Another sidelobe, at 0.43 degrees previously detected at 39 GHz, has been shown to be caused by rays reflected from that part of the prime focus box which projects beyond the edge of the subreflector (Figure 15) [4]. It has the shape of an irregular ring (the reflecting surface is not accurately plane and exhibits periodic deformations). It was been measured at 39 GHz in 1993 (Figure 22). But in December 2000 the offending surface was replaced by a section of cone,

tilted by 20 degrees, to shift the sidelobes about 3.5 degrees from boresight. The amplitude of any residual at 0.43 degrees to boresight is unknown and is likely to be very small.

Table 2 serves to summarise the results of the analysis. It lists scan number, elevation of observation, elevation offset between telescope beam and satellite. When a fit has been made (indicated by *) this is the telescope elevation offset found in fitting the model to the observed antenna temperature as a function of time. Columns 4 and 5 give the peak antenna temperature in the two orthogonally polarised receivers, normalised to 1 MHz bandwidth. A "**" indicates that the value is based on 100 KHz resolution observations. The total power corresponding (Stokes I) is in column 6. The model absolute gain at the offset of column 3 is given in column 7. The predicted power received in an isotropic antenna (gain 0 dBi) follows. From these two values the predicted power received by the model can be calculated. The difference observed - predicted power is listed in the last column.

TABLE 1 Summary of results of Cloudsat observations

Date U.T.	Scan	Az/EL (Tel.)	Az/EL (JPL)	Az/EL (clsat)	Diff. (deg)	Scan (")	Sample (sec)	Res.	T(K)
19/07	4	261.000		288.927		720	0.5	4M	≤ 0.5
13.59		38.000		38.390	0.390			1M	
20/07	6	100.300	100.37	100.495		120	0.1	4M	≤ 0.5
02.01		55.000	54.17	54.035	0.965			1M	
20/07	71	72.600	72.53	72.263		120	0.1		≤ 1
13.05		46.200	46.10	46.063	0.137				
21/07	9	287.000	286.77	281.784					CRASH
02.44		52.000	51.77	51.724	0.276				
21/07	96	268.980	258.99	258.563		20	0.1	1M	3
13.47		61.070	61.16	61.016	0.054				
22/07	7	98.530	98.63	98.525		20	0.1		≤ 0.5
01.49		39.699	39.80	39.574	0.125				
23/07	33	284.900	284.91	284.390		20	0.1	4M	
02.31		70.700	70.41	70.599	0.101			1M	3
23/07	159	256.850	257.16	256.222		10	0.05	100K	870
13.35		82.900	82.920	82.999	-0.099				
24/07	20	96.760	96.76	96.761			0.05	100K	3?
01.36		29.570	29.54	29.432	0.138				
24/07	146	68.790	68.79	68.784		10	0.05	100K	≤ 1
12.40		26.310	26.31	26.160	0.150				
25/07	26	103.080	103.80?	104.006			0.05	1M	600
02.19		85.920	85.92	86.017	0.097				
25/07	99	75.330	75.33	75.732			0.05	100K	80
13.22		73.490	73.49	73.366	0.124				

TABLE 2 Analysis of Cloudsat observations

Scan	El	Offset	1M1	1M2	Obs Power model	Gain at 0 dBi	Mean Power	Diff
	Deg.	Deg.	(K)	(K)	dBW	dbi	dbW	dB
4	38	0.390	$\leq .5$	$\leq .5$	≤ -172	+25	-192	≤ -05
6	55	0.965	$\leq .5$	$\leq .5$	≤ -172	+20	-190	≤ -02
7	40	0.125	$\leq .5$	$\leq .5$	≤ -172	+40	-192	≤ -20
20	29	0.138	?**	4**	-162	+45	-194	-13
26	86	0.049*	600	25	-141	+55	-194	+6
26	86	-0.430*	87	60	-147	?	-194	?
		+0.430*	165	70	-145	?	-194	?
		-3.200*	26	17	-152	+15	-194	+26
		+3.200*	3	5	-160	+15	-194	+18
33	70	0.101	3	1	-162	+40	-189	-13
71	46	0.137	≤ 1	≤ 1	≤ -166	+35	-191	≤ -10
96	61	0.054	3	2	-161	+45	-190	-15
99	73	0.129*	80**	47**	-143	+40	-189	+06
159	83	0.049*	205	370	-142	+40	-179	-03

There is a large scatter in this difference. It is displayed graphically in Figure 30. Since the model is expected to be worst case we expect the values of the difference to be negative. However some large positive values are found, particularly at high elevations and for responses identified (correctly ?) with spillover and reflections from the subreflector and its package. Above about 80 degrees elevation uncertainties in the pointing of the satellite beam become important. Can these account for the observations ? Another uncertainty is in the model for the 30m response in the region of the first few sidelobes - at 39 GHz there appears to be an extended region around the main beam with enhanced gain - see Figure 22. The best fits of Figures 16 to 18 give underestimates for the expected signal of up to 10 dB !

5 SATURATION

The predictions of the average power at the terminals of the 30m telescope as calculated from the model for the envelope of the sidelobes are given in Figure 28. This plots average power (dBW) as a function of satellite elevation and offset from the 30m boresight. In this case, at

angles from boresight greater than 0.7 degrees, the ITU Rec. 509 model has been used, and a simple fit to the transmitter beam (Figure 6) was adopted. The two patterns are illustrated in Figure 29. The onset of saturation in spectral observations will occur when this power exceeds the system noise in a channel of 300 kHz bandwidth. All narrower channels will be simultaneously saturated. For a system temperature of 150K this limiting power is -152 dBW. This leads to saturation for a power of -145 dBW, assuming (rather arbitrarily) that saturation sets in when power is +7 dB above system noise. Typical line observations may employ less than 300 kHz resolution. Hence if tuned in the band occupied by Cloudsat, saturation of the IF chain will occur for offsets from the satellite $\leq$ 1 degree and at high elevation $\geq$ 80 degrees). Observations with channel bandwidths greater than 300 kHz will be correspondingly less prone to saturation.

Since the SIS mixer front end does not have much frequency selectivity, the Cloudsat emission may saturate the mixer when observations are made anywhere in the 3mm band. At high power levels, when the satellite signal power is comparable with that of the local oscillator, intermodulation products may lead to false spectral features. The formulae of Kerr [3], give about 6nW (-86 dBW) as the local oscillator power typically used at 100 GHz (2 junctions, conversion gain 0.25, impedance 50 ohms). Thus we may expect intermodulation to begin at an interference power significantly smaller than -86 dBW at the mixer input.

At lower interference levels significant gain compresion will be manifest. For example from Kerr's result a 1 percent compression will occur at interference levels 20 dB lower IE at receiver input power of -106 dBW. From Figure 28 we see that for elevations less than about 80 degrees and offsets from boresight greater than a fraction of a degree, no problem will arise. This remains true even for the pulsed power, greater by 20 dB !

6 CONCLUSIONS.

To avoid receiver damage it suffices to avoid pointing near Cloudsat when it is close to the zenith. The peak power received is then about -6dBW, which exceeds that estimated for destruction (-13 dBW to -20 dBW). In principle a zenith offset of 5 degrees gives -60 dB attenuation and is largely sufficient for protection, otherwise and when the telescope is stowed at the zenith, the vertex shutter should be closed.

Figure 28 shows that saturation of the IF chain itself (at -145 dBW) is unlikely since even at 300 kHz bandwidth, elevations of $\geq$ 80 degrees and pointing offsets $\leq$ 0.1 degree are necessary ! Gain compression of 1 percent in the SIS mixer is expected at -100 dBW input power, and intermodulation at -80 dBW only.

The most likely scenario for interference is thus when the Cloudsat IF signal falls within the passband of the spectrometer - when observations are made in the shared band. The most vunerable cases occur when the frequency resolution matches that the of transmitter signal ($\leq$ 300 kHz) and for short integration times (less than a second) which allow the transit through the telescope beam to be resolved. The detection limit is then about -165 dBW with integration times of 0.1 second. Longer integration times will have a higher threshold. From Figure 26 we see that such power levels are only reached for elevation angles greater than about 80 degrees

and angles from telescope boresight less that about a degree. Strictly speaking interference can occur at all telescope elevations when the satellite is within 2 degrees of the zenith when less than about 15 seconds observing time is lost. If the signal does not fall within the passband then immediately one gains a factor in rejection of more than 40 dB at 10 MHz offset and interference is effectively impossible.

The relative probability of these different scenarios may be assessed from the data given in Table 3. It is based on about 6 months predictions (175 days) made from the orbital elements published daily by Colorado State University. It therefore takes into account any inaccuracies in station keeping. Such uncertainties are displayed graphically in Figure 29, where a scatter of a fraction of a degree in maximum elevation and about 1 minute in time were predicted for a 6 month interval in 2007.

TABLE 3 Overpass Statistics, Pico Veleta June-December 2007.

Elevation range (degrees)	Number in 175 days
≥ 87.5	10
≥ 85.0	11
≥ 82.5	21
≥ 80.0	22
≥ 77.5	33
≥ 75.0	36

Thus the key factors rendering interference unlikely during routine observations are the very low transmitter sidelobes in both angle and frequency (Figures 4, 5 and 6). It suffices for example to restrict observations to satellite elevations less than 82 degrees, with telesope pointing offset by more than about a degree (Figure 28) from the satellite. Other combinations are possible of course such as elevation ≤ 85 degrees but with pointing offsets restricted to ≥ 10 degrees. In all cases the adverse effects are expected to last only a few seconds typically.

Simple guidelines (Figure 4) can be made if observations are restricted to times when Cloudsat is below 82 degrees elevation. Then coupling is to the transmitter sidelobes (at -75 dB) and additional protection is given by the offset between satellite and boresight directions.

In this special case (time) sharing between Radioastronomy and an active service is feasible at the price of some loss in observing time. This is possible because only one fast moving satellite with excellent sidelobes in angle and frequency is active.

TABLE 4 Guidelines when Cloudsat elevation $\leq$ 82 degrees

Effect	Input Power (peak dBW)	Extra Rejection Needed	Telescope gain (dBi)	Offset Needed (degrees)
SIS				
non linearity	-86	-5	+81	0.1
1 compression	-106	-25	+61	0.5
Inband IF				
Saturation	-152	-71	+15	5
Interference	-165	-82	+4	12
	-183 mean			

7 ACKNOWLEDGMENTS.

Thanks are due to the director and staff at Pico Veleta for their hospitality and help.

References

[1] Stephens G.L., et al.,"The Cloudsat mission", Bull. American Meteorological Society, **83**,(12) pp. 1711-1790, December 2002

[2] Durden S., and Boain R. "Orbit and Transmit Characteristics of the Cloudsat Cloud Profiling Radar", JPL Document No. D-29695, Pasadena CA 91109, 26 July 2004 (revised 2 September 2004)

[3] Kerr A.R.,"Saturation by Noise and CW Signals in SIS Mixers", ALMA Memo. 401, 14 December 2001 (revised 5 April 2002): 2002 International Symposium on Space THz Technology, Cambridge MA, March 2002

[4] Hills R.,Private communication 1993

[5] Penalver Juan, IRAM May 2006

[6] Magliacane John A., KD2BD, kd2bd@amsat.org

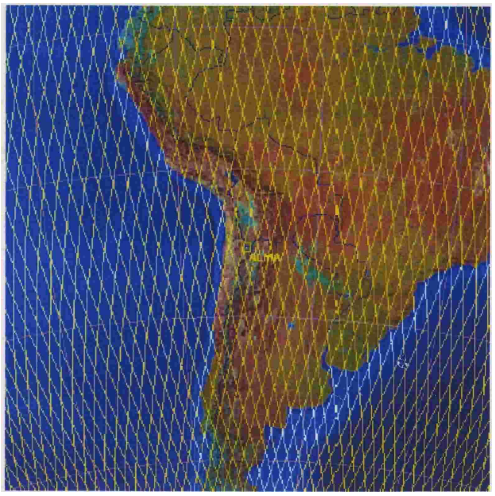

Figure 1: An example of the Worldwide Reference System grid over South America. The ascending S-N orbits slope from lower right to upper left, the decending orbits (N-S) slope from upper right to lower left.

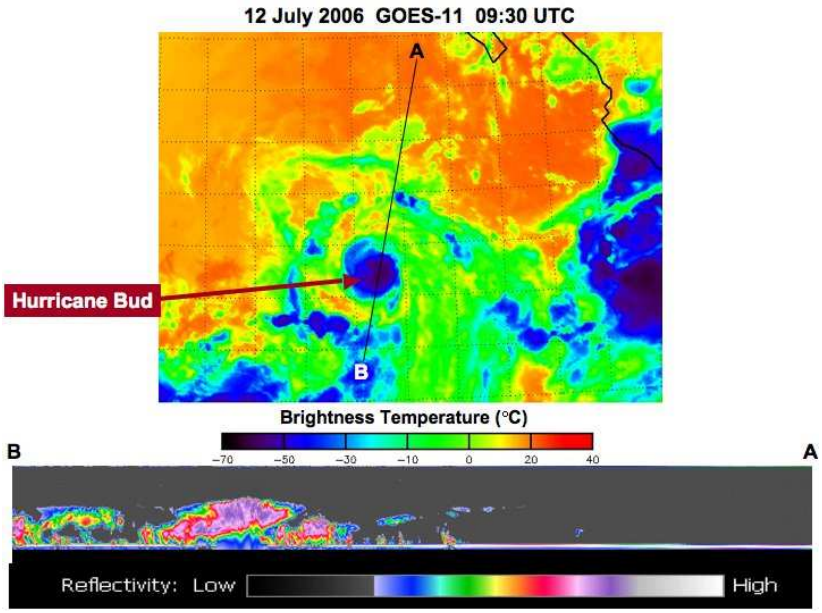

Figure 2: Cloudsat observations of hurricane Bud.

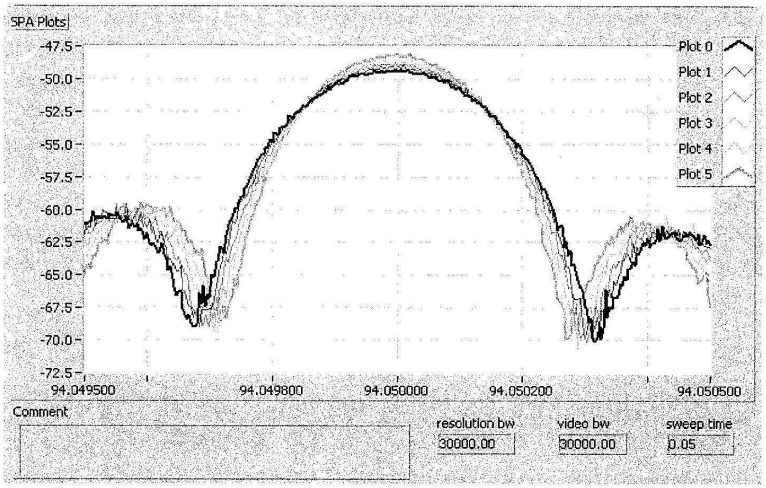

Figure 3: Measured spectrum of the Cloudsat emissions.

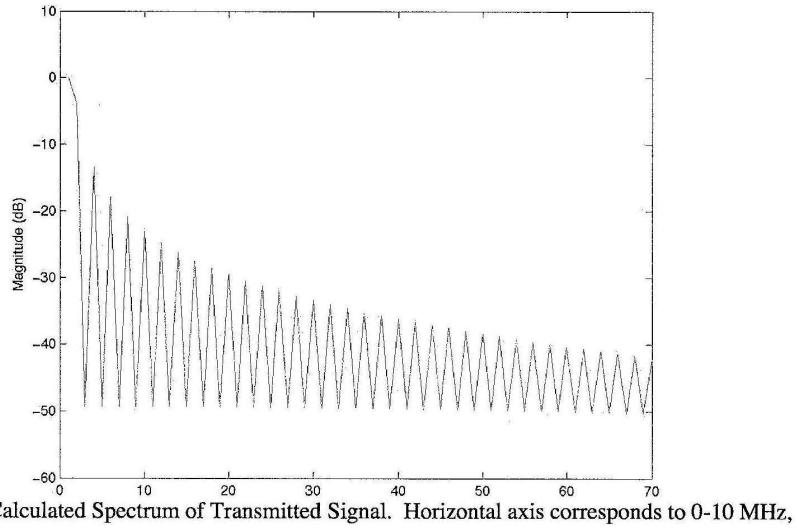

Figure 4: Predicted spectrum of Cloudsat calculated from the measured rise and fall times of the pulses.

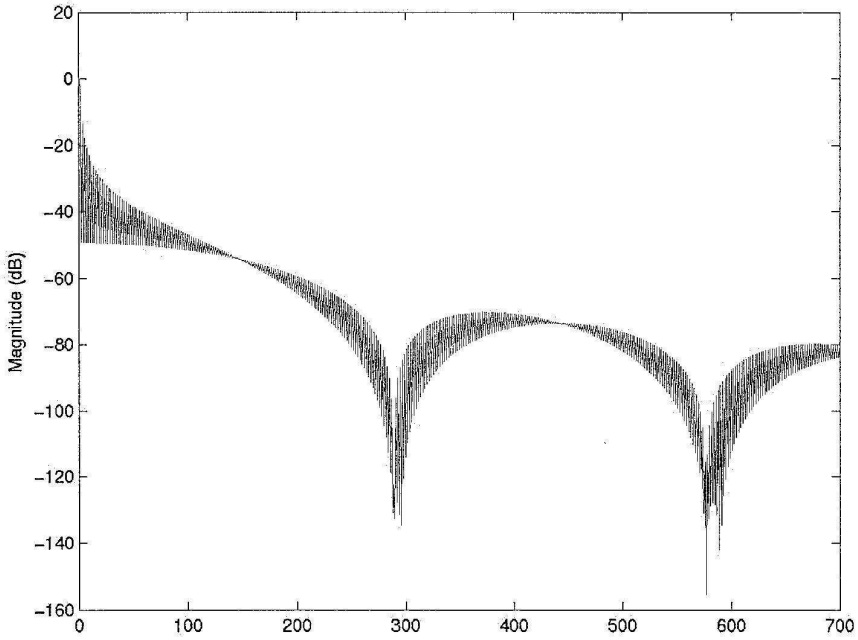

Calculated Spectrum of Transmitted Signal. Horizontal axis corresponds to 0-100 MHz, approximately.

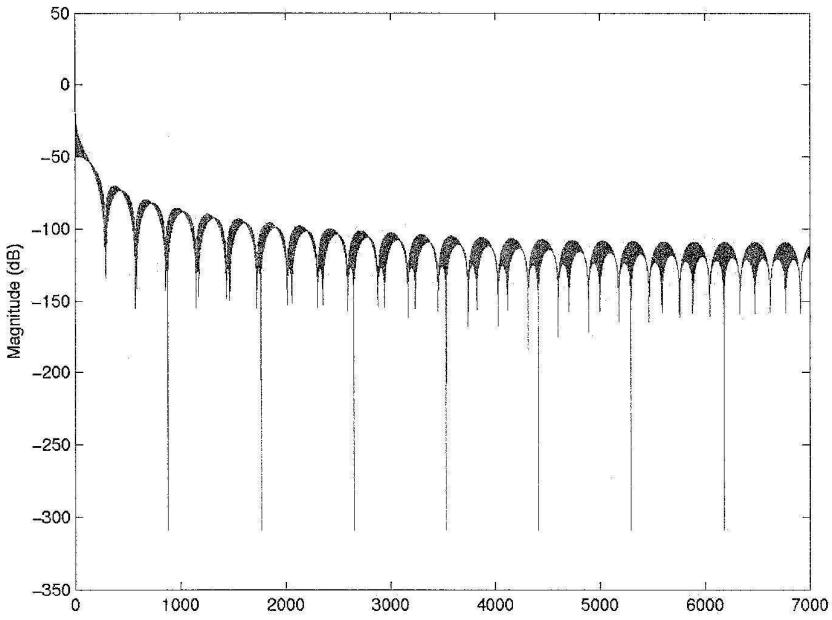

Calculated Spectrum of Transmitted Signal. Horizontal axis corresponds to 0-1 GHz, approximately.

Figure 5: Predicted spectrum of Cloudsat calculated from the measured rise and fall times of the pulses.

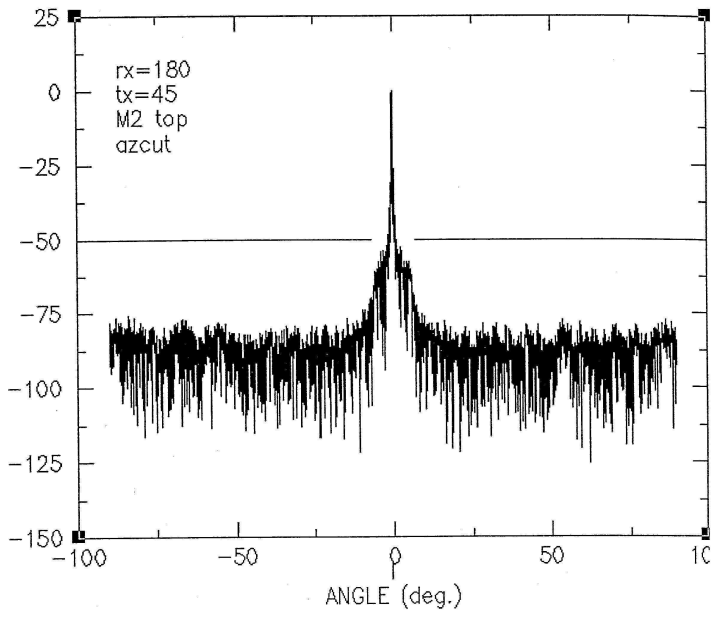

Figure 6: Far field sidelobe pattern of the Cloudsat radar - deduced from near field laboratory measurements.

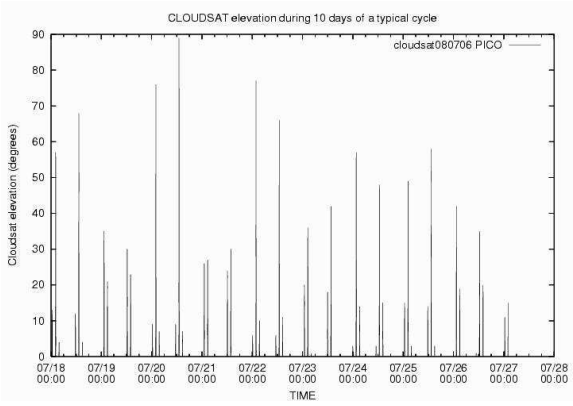

Figure 7: Cloudsat elevation during a typical 10 days period at Pico Veleta.

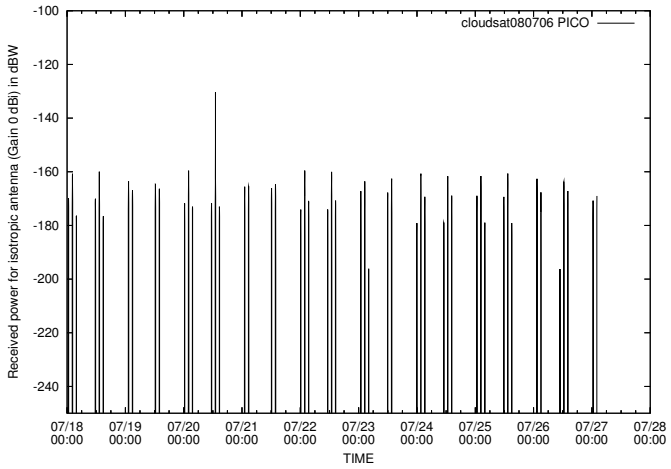

Figure 8: Peak power received in isotropic antenna (gain - dBi) - for 10 days one cycle.

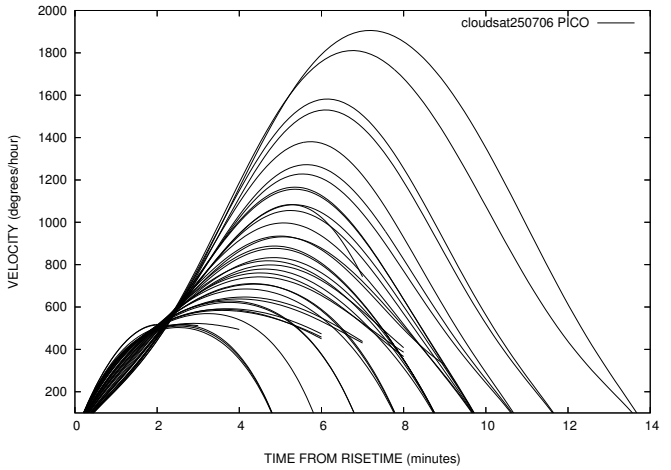

Figure 9: Angular velocity of Cloudsat calculated from "Predict" as a function of time from risetime during a typical cycle of 233 orbits.

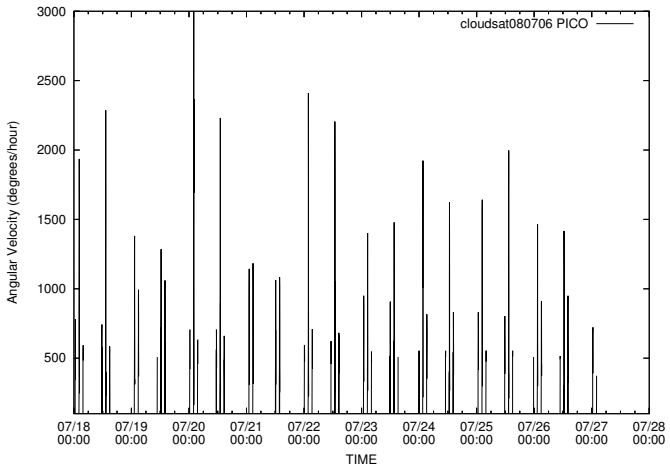

Figure 10: Angular velocity of Cloudsat calculated from "Predict" as a function of time during a typical part (10 days) of a 16 day cycle.

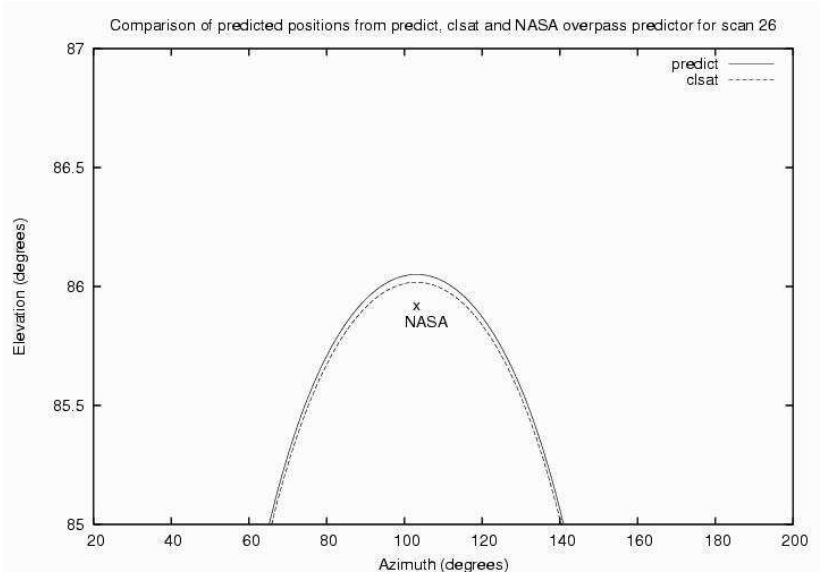

Figure 11: Comparison of the predicted path of Cloudsat according to "predict" and "clsat" - pass Scan 26, 25 July 2006.

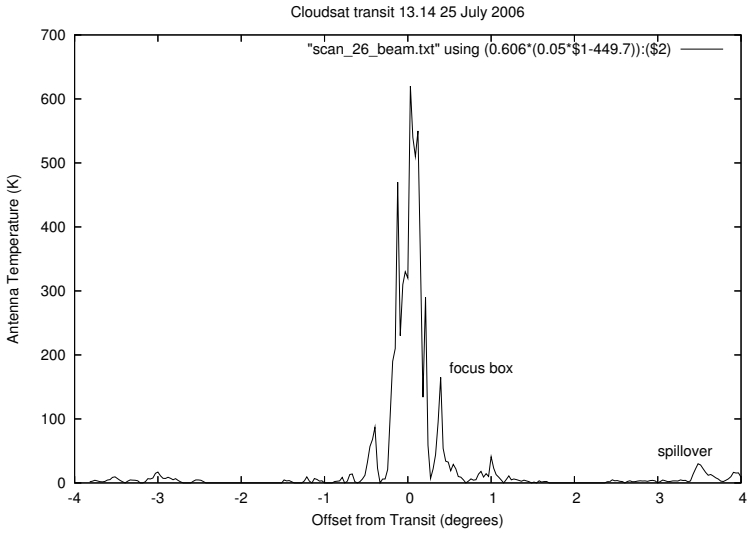

Figure 12: Observed power at 94.05 GHz versus time, Scan 26, 25 July 2006. Abscissa labelled in azimuth offset from boresight. Sample time 0.05 second.

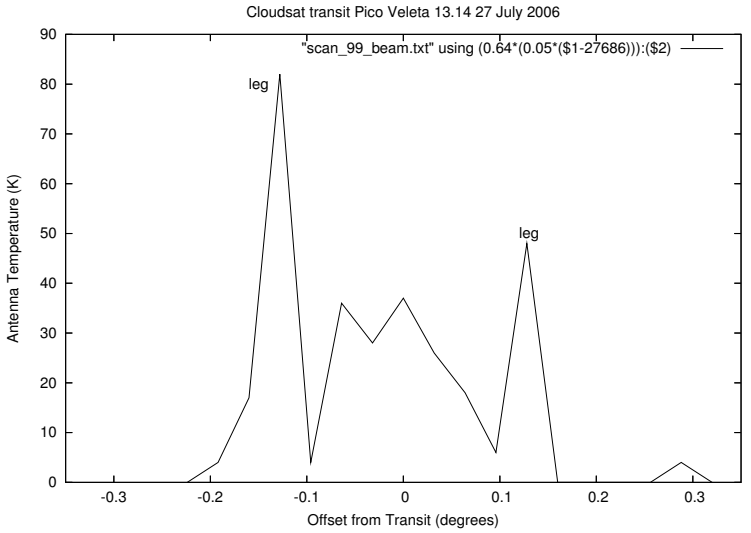

Figure 13: Observed power at 94.05 GHz versus time, Scan 99, 25 July 2006. Abscissa labelled in azimuth offset from boresight. Sample time 0.05 second.

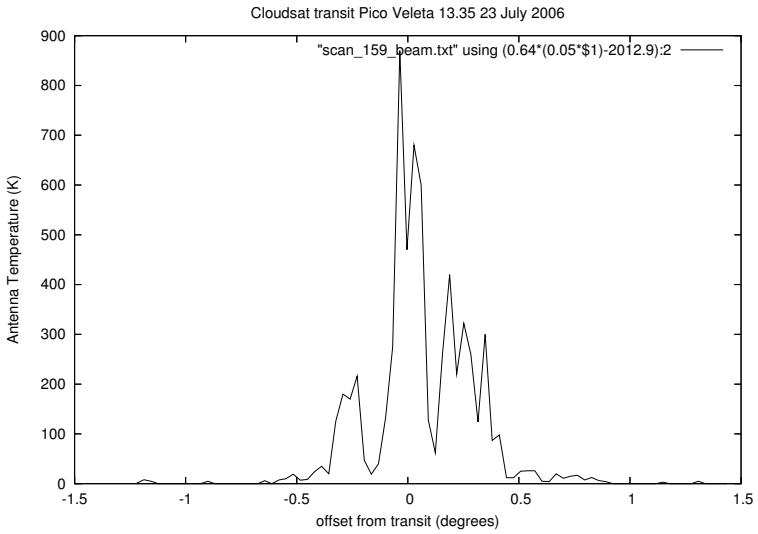

Figure 14: Observed power at 94.05 GHz versus time, Scan 159, 23 July 2006. Abscissa labelled in azimuth offset from boresight. Sample time 0.05 second. No fit has been found to explain this observation.

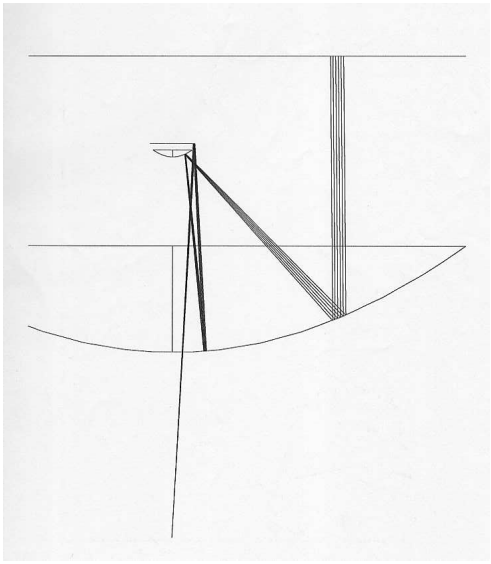

Figure 15: Path of rays reflected from the focus cabin, resulting in a sidelobe of complicated structure at 0.43 degrees from boresight [4] (see Figures 9 and 19). Configuration before December 2000.

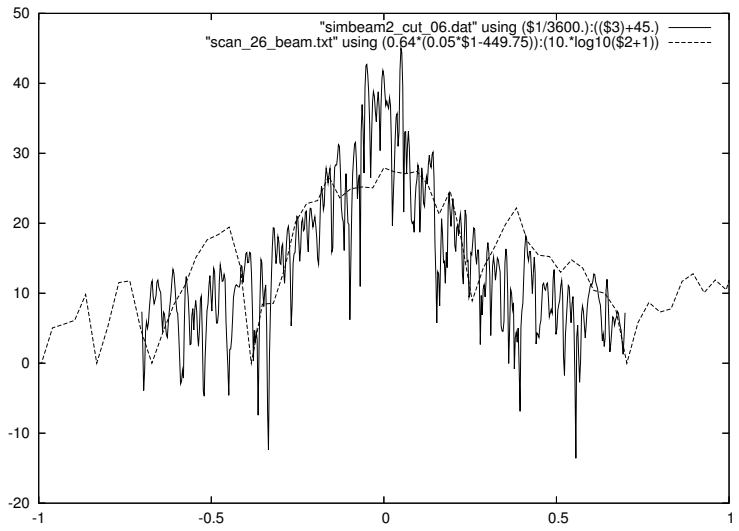

Figure 16: Scan 26, 25 July 2006 with model fit (dotted) at elevation offset 0.097 degrees. The abscissa is given in degrees of azimuth from boresight, ordinate (K). Sample time 0.05 second.

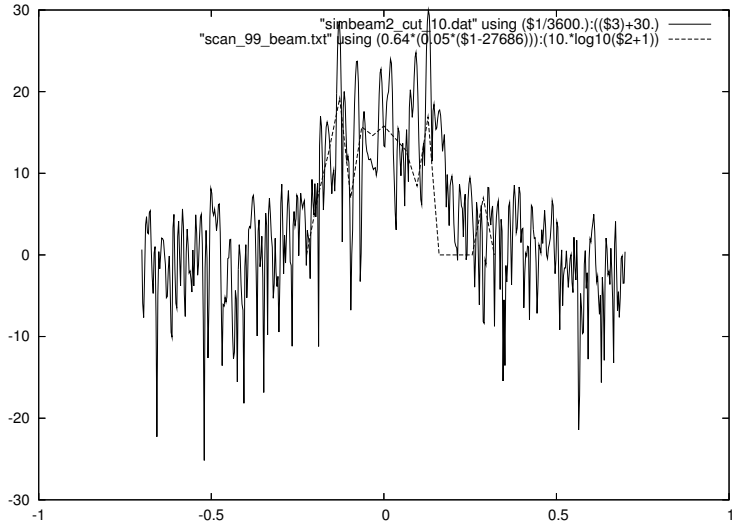

Figure 17: Scan 99, 25 July 2006 with model fit (dotted) at elevation offset 0.124 degrees. The abscissa is given in degrees of azimuth offset from boresight, ordinate (K). Sample time 0.05 second.

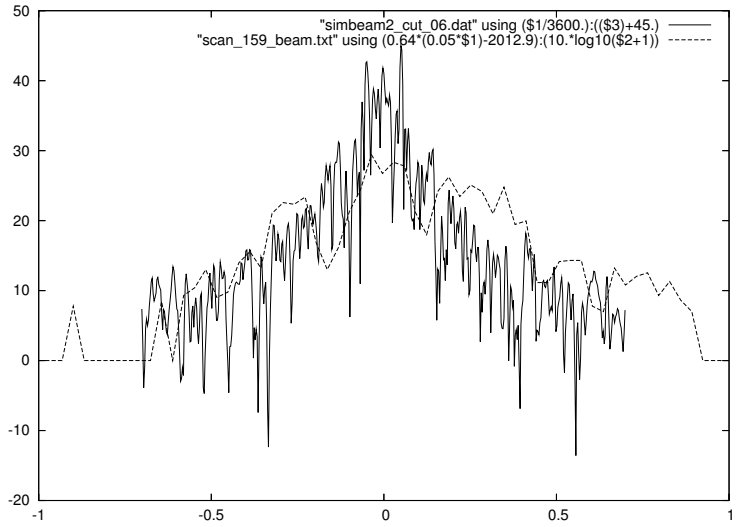

Figure 18: Scan 159, 23 July 2006 with model fit (dotted) at elevation offset 0.1 degrees. The abscissa is given in degrees of azimuth offset from boresight, ordinate (K). Sample time 0.05 second.

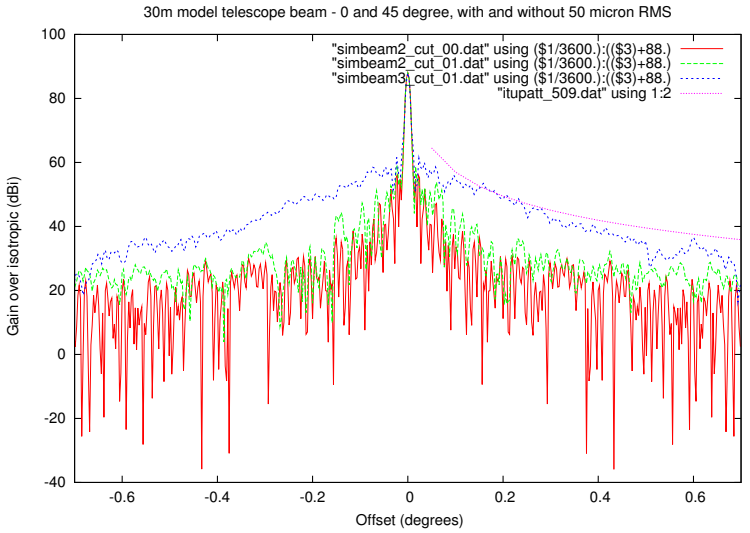

Figure 19: Comparison of model predictions for cuts through the 94 GHz beam and the sidelobe standard of ITU Rec. S509. In increasing gain - 0 degrees (azimuth) cuts model without surface error (full line). Zero degree cut with RMS panel errorrs of 54 microns errors (small dots). With panel errors and cut at 45 degrees to azimuth direction (parallel to legs). ITU Rec. S509 (closest spaced dots between +0.05 and +0.7 degrees offset).

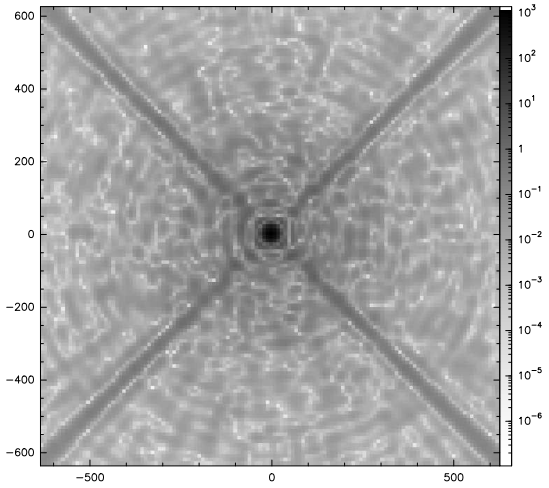

Figure 20: 94 GHz beam predicted by the model for the inner (±0.17) degrees. Angular scales in arc seconds.

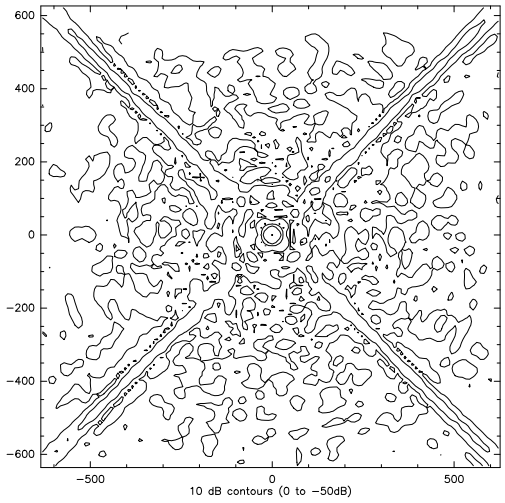

Figure 21: 94 GHz beam predicted by the model for the inner (±0.17) degrees. Angular scales in arc seconds.

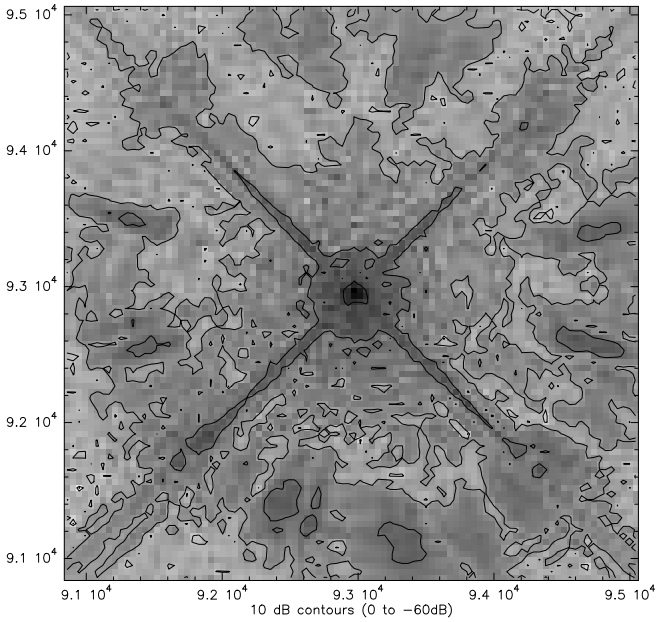

Figure 22: Polar diagram of the 30m telescope as measured in 1993 at 39 GHz before the focus box was modified. These mesurements used ITALSAT in 1993. Angular scales in arc seconds.

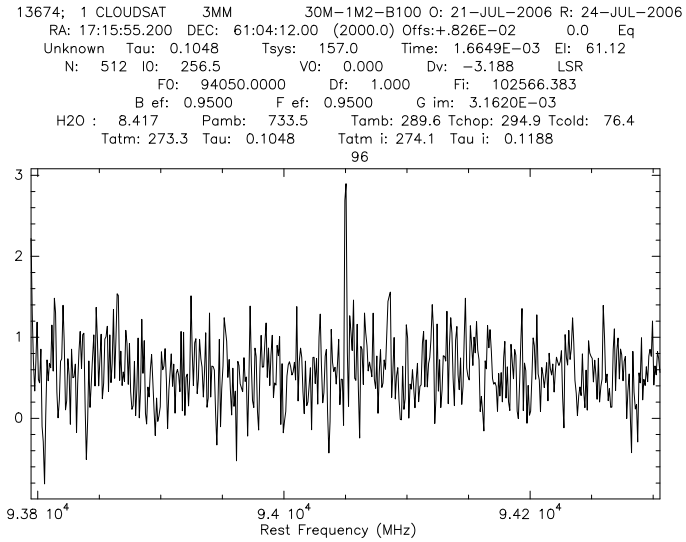

Figure 23: Scan 96, 21 July 2006, receiver B100. Ordinate - antenna temperature (K), elevation 61.0 degrees. Tel.-NASA=-0.09, Tel.-clstat=0.05.

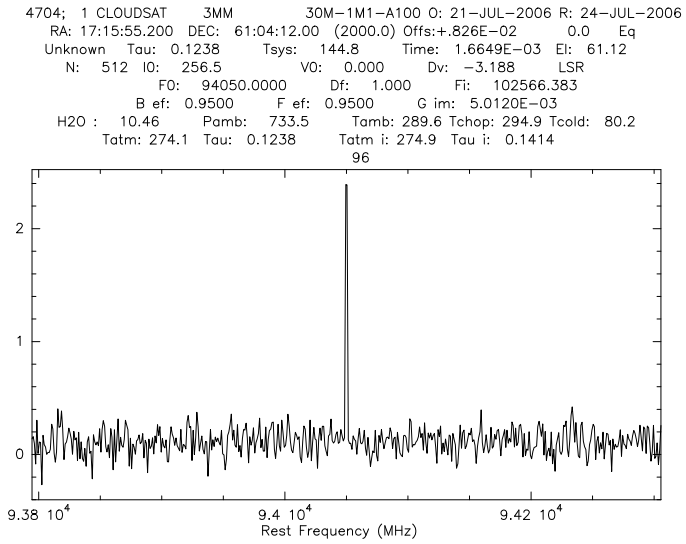

Figure 24: Scan 96, 21 July 2006, receiver A100. Ordinate - antenna temperature (K), elevation 61.0 degrees. Tel.-NASA=-0.09, Tel.-clstat=0.05.

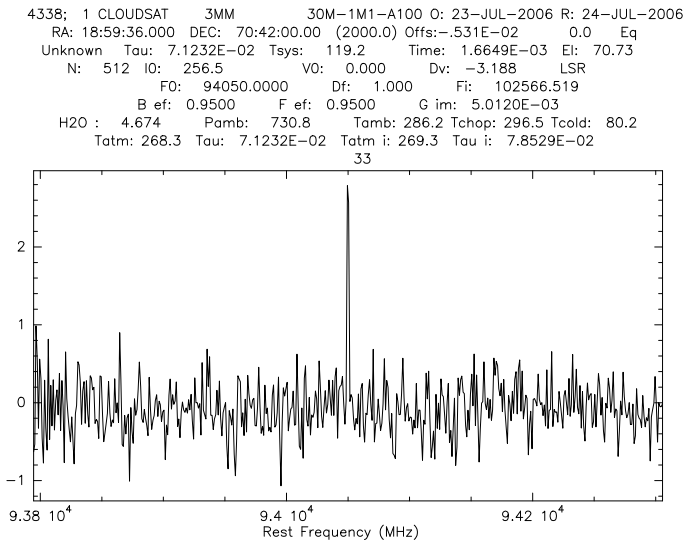

Figure 25: Scan 33, 23 July 2006, receiver A100. Ordinate - antenna temperature (K), elevation 70.7 degrees, resolution 1 MHz, Tel.-NASA=-0.01, Tel.-clsat=0.51.

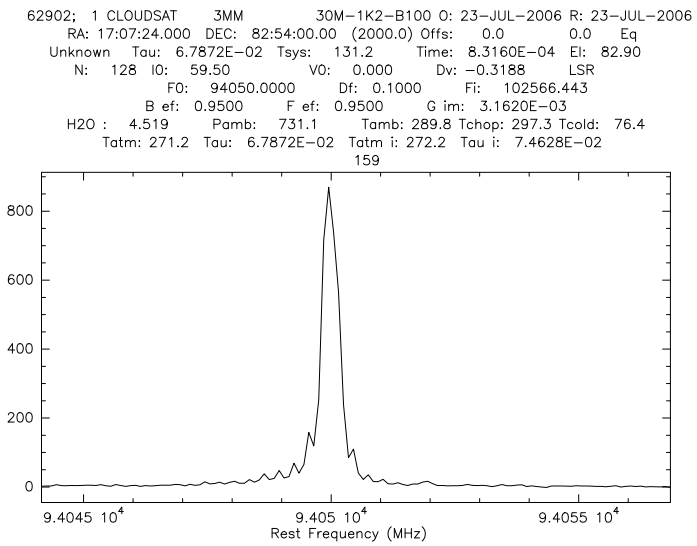

Figure 26: Scan 159 23 July 2006, receiver B100. Ordinate - antenna temperature (K), elevation 82.9 degrees. Tel.-NASA=-0.02, Tel.-clsat=-0.10.

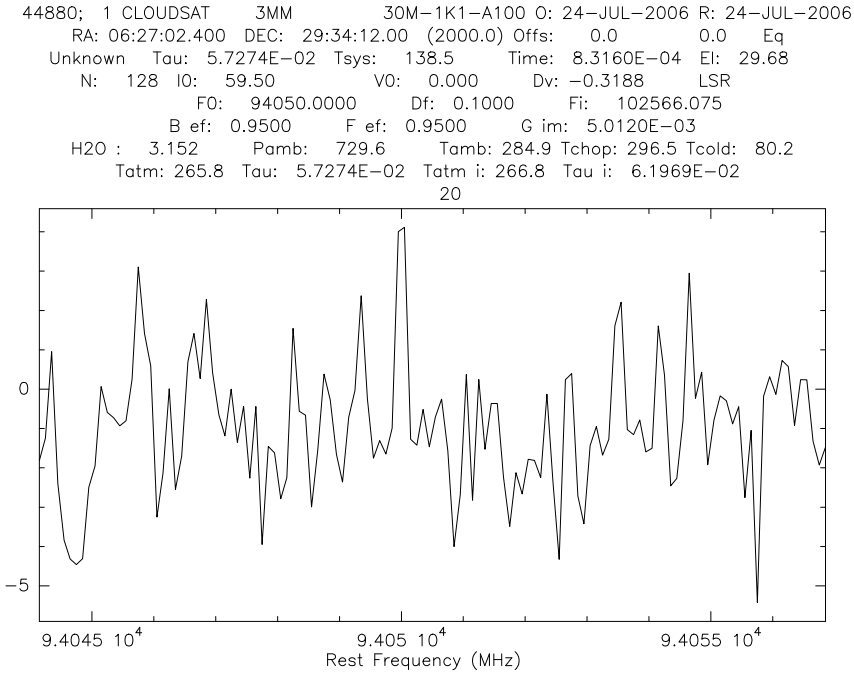

Figure 27: Scan 20, 24 July 2006, receiver A100. Ordinate - antenna temperature (K), elevation 29.6 degrees. This is the weakest signal detected.

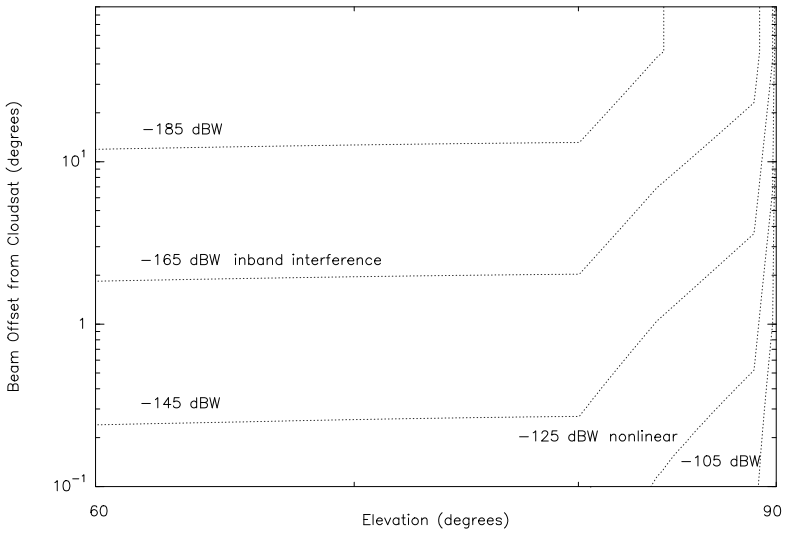

Figure 28: Upper limits to average power at input to 30m receivers (dBW) at 94.05 GHz calculated using ITU Rec. 509 for 30m sidelobes, NASA measurements for transmitter sidelobes (Figure 6) [2]. Power levels are indicated in dBW.

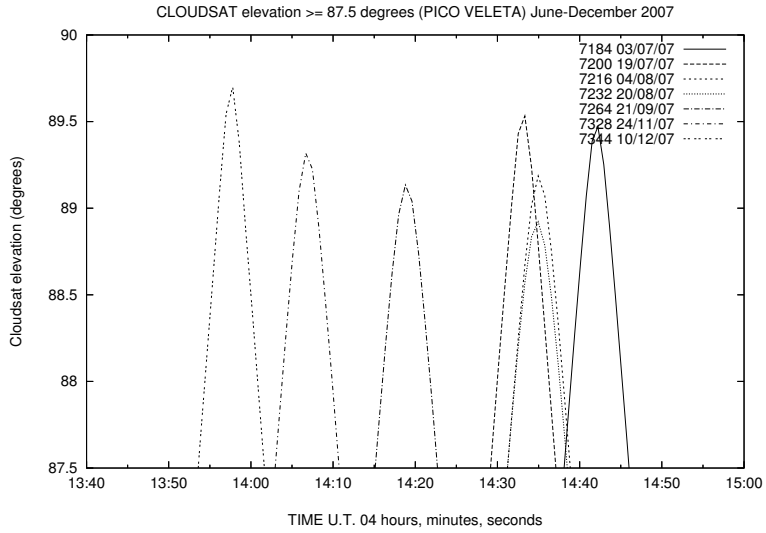

Figure 29: Predicted scatter in overpasses at high elevation ($\geq$ 87.5 degrees) during a 6 month time interval.

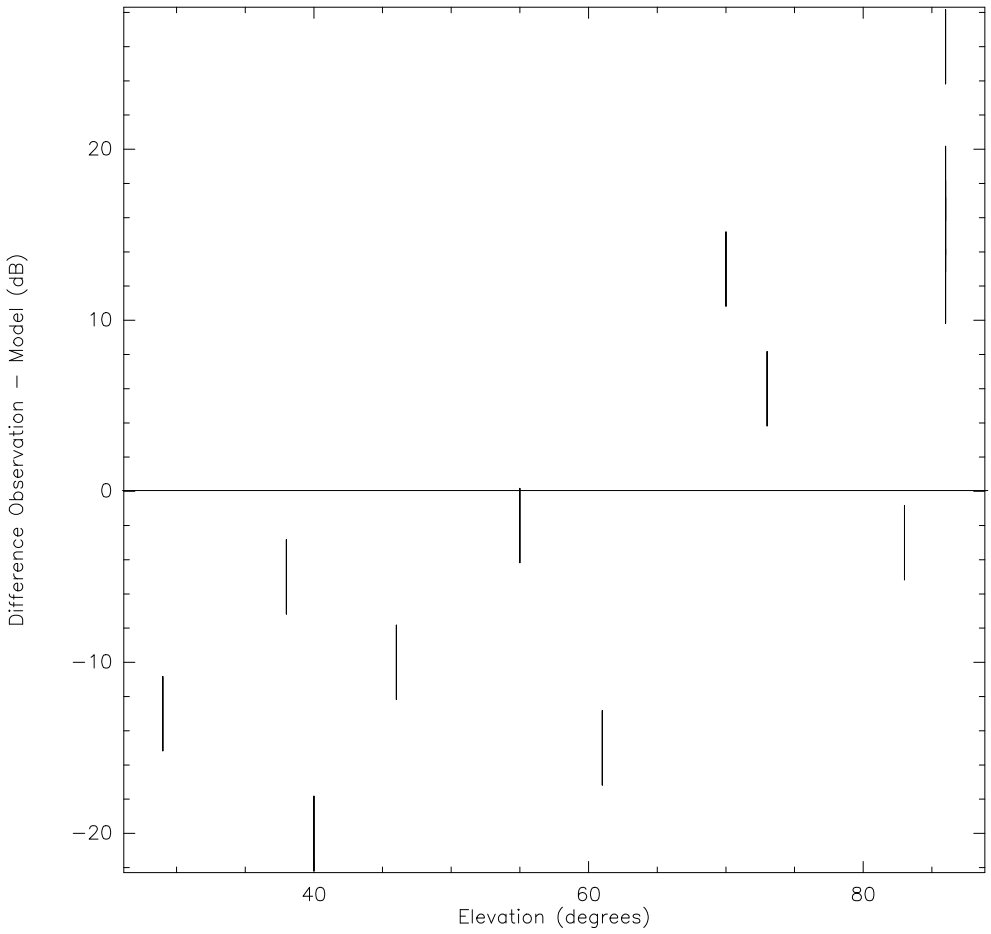

Figure 30: Comparison of observed power with that predicted by the model. The vertical bars only indicate a constant 4 dB range.